A Defects-Based Model on the Barrier Height Behavior in 3C-SiC-on-Si Schottky Barrier Diodes

Anastasios E. Arvanitopoulos, Marina Antoniou, Mike R. Jennings, Samuel Perkins, Konstantinos N. Gyftakis, *Member, IEEE*, Philip Mawby, *Senior Member, IEEE*, and Neophytos Lophitis

***Abstract*— 3C-silicon carbide (3C-SiC) Schottky barrier diodes (SBDs) on silicon (Si) substrates (3C-SiC-on-Si) have been found to suffer from excessive subthreshold current, despite the superior electrical properties of 3C-SiC. In turn, that is one of the factors deterring the commercialization of this technology. The forward current–voltage (I–V) characteristics in these devices carry considerable information about the material quality. In this context, an advanced technology computer-aided design (TCAD) model is proposed and validated with measurements obtained from a fabricated and characterized platinum/3C-SiC-on-Si SBD with scope to shed light on the physical carrier transport mechanisms, the impact of traps, and their characteristics on the actual device performance. The model includes defects originating from both the Schottky contact and the heterointerface of 3C-SiC with Si, which allows the investigation of their impact on the magnification of the subthreshold current. Furthermore, the simulation results and measured data allowed for the identification of additional distributions of interfacial states, the effect of which is linked to the observed nonuniformities of the Barrier height value. A comprehensive characterization of the defects affecting the carrier transport mechanisms of the investigated 3C-SiC-on-Si power diode is thus achieved, and the proposed TCAD model is able to accurately predict the device current both during forward and reverse bias conditions.**

***Index Terms*— 3C-SiC-on-Si, band diagram, cubic silicon carbide (SiC), inhomogeneous, Schottky barrier diode (SBD), Schottky barrier height (SBH), semiconductor device modeling, SiC, technology computer-aided design (TCAD), traps.**

Manuscript received June 10, 2019; revised August 10, 2019; accepted September 6, 2019. Date of publication September 20, 2019; date of current version February 3, 2020. This work was part of the Challenge project, founded by European Commission, ID 720827. Recommended for publication by Associate Editor Laili Wang. *(Corresponding author: Anastasios E. Arvanitopoulos.)*

A. E. Arvanitopoulos, S. Perkins, and N. Lophitis are with the Institute for Future Transport and Cities, Coventry University, Coventry CV1 5FB, U.K., and also with the Faculty of EEC, Coventry University, Coventry CV1 5FB, U.K. (e-mail: arvanita@uni.coventry.ac.uk; perkin19@coventry.ac.uk; n.lophitis@cantab.net).

M. Antoniou and P. Mawby are with the School of Engineering, Universityof Warwick, Coventry CV4 7AL, U.K. (e-mail: marina.antoniou@warwick.ac.uk; p.a.mawby@warwick.ac.uk).

M. R. Jennings is with the College of Engineering, Swansea University, Swansea SA2 8PP, U.K. (e-mail: m.r.jennings@swansea.ac.uk).

K. N. Gyftakis is with the School of Engineering, The University of Edinburgh, Edinburg EH8 9YL, U.K. (e-mail: k.n.gyftakis@ieee.org).

Color versions of one or more of the figures in this article are available online at http://ieeexplore.ieee.org.

Digital Object Identifier 10.1109/JESTPE.2019.2942714

I. Introduction

SILICON carbide (SiC) is a very promising material due to its wide bandgap (WBG) properties and has the potential to replace silicon (Si) in various power electronic applications [1], [2]. The 3C-SiC is the only cubic polytype of SiC, also found in the literature as β-SiC [3]. Other major SiC polytypes, like 4H- and 6H-SiC, feature a hexagonal structure that introduces anisotropies in their electrical properties and are generally grouped as α-SiC. Notably, power devices based on 3C-SiC inherit these isotropic electrical characteristics owned to its cubic structure [4]. Such isotropic behavior, mainly on the mobility and the impact ionization of carriers, is of significant importance for power devices [5]. In addition, the cubic SiC features a slightly smaller energy bandgap (E_g) compared to 4H-SiC that stands as a remarkable benefit for metal–oxide–semiconductor field-effect transistors (MOSFETs) by energetically locating the SiO2/3C-SiC interfacial traps in the conduction band of 3C-SiC, and in turn, resulting in a largely improved channel mobility [6]–[8]. Therefore, 3C-SiC MOSFETs are expected to have remarkably reduced conduction losses and increased reliability. Furthermore, 3C-SiC has the ability to be grown on cheap Si substrates (3C-SiC-on-Si) [9]. This allows large-area wafers of the material to be obtained and the cost for power devices fabrication to be reduced. Hence, 3C-SiC-on-Si power devices offer a cost-effective high-performance WBG technology platform where the improved devices' performance, including high-temperature operation, faster switching, and lower losses, can translate in a new generation, high-performance, and compact power electronics converters and accelerate the replacement of Si technology. The 3C-SiC-on-Si Schottky barrier diode (SBD) is a great candidate device because it combines the superior WBG material properties of SiC with the properties of SBDs such as negligible reverse recovery, low switching losses, and high operating temperatures. However, so far, the formation of a reliable pure Schottky contact on SiC has been proved as a rather challenging task, mainly suffering from high reverse leakage current [10].

The observed high leakage could be attributed to traps in bulk or at the interface between the metal and the semiconductor, some of which could originate at the heterointerface

between Si and 3C-SiC, e.g., induced by the lattice mismatch between the two materials [9], [11]. The presence of these defects and the high leakage is considered a bottleneck, hindering the commercialization of this technology [12]–[14]. Recent developments in the heteroepitaxy process [15]–[18] suggest that 3C-SiC epilayers with low bulk defect densities can soon be obtained yet a better understanding of the causes of this leaky behavior is needed as well as the location and type of defects and traps. An SBD is indeed an ideal test device for the study of the carrier transport mechanisms in any semiconductor material, the related physics, and the impact of traps on the aforementioned. An appropriate model that can include those would allow to reach a deep level of understanding of these complex phenomena and would stand out as a significant milestone for the creation of accurate designs, which could in turn suppress the currently observed excessive leakage and subthreshold current levels [19]–[21].

However, interfaces formed when SiC is brought into contact with metals are rather complex carriers' transport systems [22]. The Schottky—Mott rule [23] is hardly ever observed in experiments because it omits the impact of interface states and charges on the actual Schottky barrier height (SBH). In addition, evidences of SBH inhomogeneity [24] discourage the adaptation of the Fermi level (E_F) pinning mechanism in explaining why the Schottky–Mott theory lacks in accuracy.

The inhomogeneity of the Schottky contacts has been widely investigated for the SiC SBDs. Nonuniform properties of the SBH create the conditions for an increased leakage current and a reduced blocking voltage value [25]. In [26]–[28], such variations in performance have been attributed to the existence of a Gaussian distribution for the SBH values around a mean value. Another simplistic approach suggests two independent SBHs in parallel [29]–[31] to express the resultant current. Inhomogeneous Schottky contacts have also been described by Tung's model [25], [32]. According to this model, spatially, no uniformities of the barrier height are related to potential fluctuations at the Schottky interface-forming patches. The patch dimensions are comparable with the space charge region width. Therefore, in low forward-bias conditions, the conducting low-barrier patches have their current laterally pinched-off. Nonetheless, this fitting model is not applicable for diodes with a significant degree of nonideality ($\eta > 1.21$) [30]. Furthermore, the physical interpretation of these fitting parameters remains mainly unanswered [33].

Interestingly, it has been shown that the inhomogeneity of the SBHs can be linked with the presence of defects of various origins, including both the materials and the devices [34]–[39]. In [40], defect clusters spatially located near the Schottky interface were responsible for the formation of partial low-barrier patches. Different SiC SBDs have been characterized in [41], with the existence of varying degrees of deep levels that were identified as the cause for the observed differences in the leakage current. However, the physical mechanisms of these traps' influence on the barrier height of SiC SBDs are still mostly unclear.

In this article, a model is developed based on interfacial traps, which obey conditional trapping/detrapping rules, to describe the behavior of the SBH in Schottky metal/3C-SiC-on-Si interfaces. Advanced technology computer-aided design (TCAD) is utilized along with measurements from a fabricated and characterized vertical 3C-SiC-on-Si SBD [42], establishing a deeply physical method, which allowed to link the nonuniformities of the SBH with the impact of traps. Thereafter, a comprehensive model is suggested to accurately describe the observed excessive leakage currents in both forward and reverse operations. The model is built upon the presence of trap states at the Schottky interface, and the physics governing their effect on the carrier transport mechanisms are revealed. It is, therefore, considerably more accurate to existing models, especially when the η value of SBDs exceeds unity.

According to the proposed TCAD model, the interfacial traps' dynamics can introduce a nonuniform distribution of the electric field at the surface of the Schottky contact. Such a condition is likely to enhance mechanisms like the image force lowering of the SBH, field emission (FE) or quantum barrier tunneling mechanism, and trap-assisted tunneling (TAT). This can significantly modify the number of carriers having the required kinetic energy to cross the barrier and, in turn, strongly affects the subthreshold current. Moreover, in the postthreshold region, the forward current mainly depends on the thermionic emission (TE) theory and is directly affected by the discrete bulk deep levels. Consequently, in this article, a complex contribution is modeled, which indirectly influences the barrier height and the resistivity, in accurately reproducing the subthreshold, the ON-state and the leakage current obtained by measurements.

The rest of this article is organized as follows. In Section II, the physics-based theory of the proposed TCAD model is presented. In Section III, the model is applied and validated utilizing measurements from a 3C-SiC-on-Si SBD. Finally, in Section IV, the conclusions of this article are presented.

II. Suggested Model for the Subthreshold Current With the Impact of the Schottky Interface States

The terms defect, trap, and state are referenced throughout this article. A "defect" is a generic term used to reference material anomalies responsible for the formation of traps. The term "trap" specifically refers to the energy level that exists due to a defect of the crystal lattice and is able to conditionally capture charge carriers, temporarily or permanently. Traps can be of donor and/or acceptor type. The term "state" indicates a trap spatially located at the metal/semiconductor interface demonstrating donorlike and/or acceptorlike behavior.

A. Linking the Interface States With a Uniform Behavior of the Schottky Barrier Height of the Schottky Contact

In 3C-SiC SBDs, the TE theory predicts a low subthreshold current in forward bias. For each temperature value, only a fraction of majority carriers from the tail of the resulting occupation distribution features enough energy to overcome the Schottky barrier. However, elevated subthreshold current levels are usually observed in fabricated devices. The main

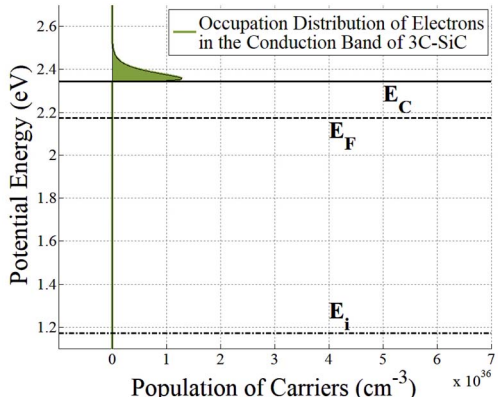

Fig. 1. Occupation distribution of the electrons in E_C of 3C-SiC as resulted from the multiplication of the probability of occupation of state (Fermi–Dirac distribution) with the number of available density of states in this band [43]. The calculations refer to a 1.5 x10^{16}cm^{-3} n-type-doped material and T = 300 K. The zero potential energy in this illustration corresponds to the valence band (E_V) of 3C-SiC.

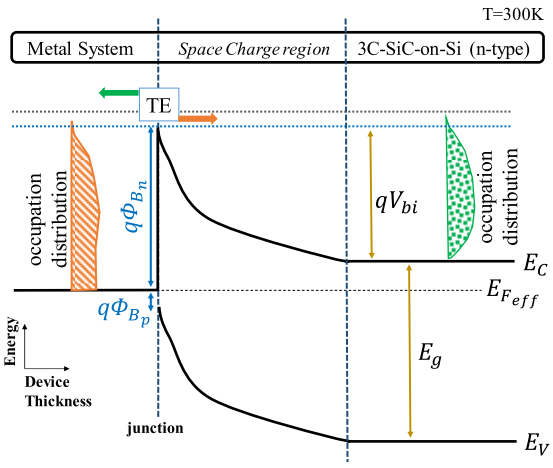

Fig. 2. For a defect-free metal/3C-SiC-on-Si interface in equilibrium and for a specific temperature, the TE predicts a small amount of carriers from the 3C-SiC occupation distribution in E_C to be able to cross the barrier.

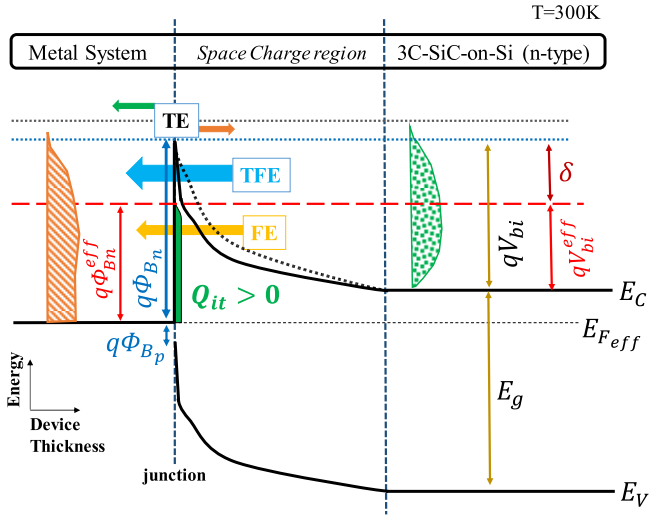

Fig. 3. Interfacial donorlike states can modify the equilibrium conditions enabling a greater portion of the electrons' occupation distribution to cross the barrier, thus resulting in more current in early forward bias. The dotted E_C represents the initial bending due to the depletion region without any effect from interfacial states.

reason for this is the combined effect of both the Schottky interface and the bulk 3C-SiC defects. For a given temperature, the kinetic energy of the majority carriers remains unaltered and so does the shape of the occupation distribution in the conduction band. Thus, the observed high level of the subthreshold current indicates that the presence of traps should introduce an effect on the potential energy at the interface affecting the SBH value. This essentially modifies the ratio between the number of majority carriers able to cross the barrier and their total population at a specific temperature in the occupation distribution. Therefore, a TCAD model is proposed to imitate the impact of the traps and states existing in a 3C-SiC-on-Si SBD on the SBH value and, in turn, the overall electrical performance.

For the rest of this article, we assume n-type 3C-SiC-on-Si material and, thus, electrons as the majority carriers. The authors previously reported on the parameters and physical models of the bulk 3C-SiC aiming for representative TCAD modeling and simulation [43]. Utilizing this material physical model, the occupation distribution of electrons in the conduction band (E_C) of the 3C-SiC is illustrated in Fig. 1.

With the suggested TCAD model, the subthreshold region of the forward $\log(I)$–V characteristics of an SBD is utilized as a starting point. This region has been linked with the quality of the material [44], allowing, therefore, for the various trap distributions to be identified. The identified traps can act either as recombination or generation centers depending on the bias conditions. An illustration of the band diagrams for a 3C-SiC-on-Si SBD is shown in Fig. 2 for the case where no interfacial defects are considered. The TE theory predicts a specific amount of majority carriers from the occupation distribution, having the required energy to flow to the metal side.

In equilibrium, this current is balanced by the occupation distributions at the conduction bands of each system. Nonetheless, the existence of states at the Schottky interface disrupts this thermal equilibrium condition.

In this section, we assume the Schottky interface to feature a trap profile comprising donor and/or acceptorlike states. Each type of these interfacial states is considered to have a continuous energetic distribution over a specific range of energies. The neutrality level (E_0) level separates the acceptor from the donor levels. Traps energetically located below E_F are more likely to carry an electron. On the contrary, the ones above E_F are more likely to carry a hole. The acceptor traps carrying a hole are neutral, while they become charged (negatively) after capturing an electron. Similarly, donor traps carrying an electron are neutral unless they are occupied by a hole that makes them charged (positively). Hence, the fixed position of the traps' E_0 and the position of E_F, which varies with the applied voltage [45], essentially determine whether there exists additional charge and of what polarity at the Schottky interface.

Fig. 3 illustrates a case where the interface traps' profile consists of a continuous band of donorlike states. The donor

states energetically above E_F can become occupied, forming a positive charge at the interface, the Schottky barrier becomes thinner, and an effective build-in potential ($V_{\text{bi}}^{\text{eff}}$) is formed. The difference between the actual build-in potential (V_{bi}) and $V_{\text{bi}}^{\text{eff}}$ can be seen in Fig. 3 as delta (δ). Notably, $V_{\text{bi}}^{\text{eff}}$ depends directly on the quantity of ionized occupied states. Under zero bias, there exists an increased quantity of majority carriers crossing the barrier because of thermionic FE (TFE). FE current is also present and its importance depends on the concentration of these states.

The application of small forward bias (V_f) moves all bands, including E_F upward. This upward movement of E_F reduces the quantity of occupied donorlike states. Consequently, the positive charge at the interface reduces, which, in turn, decreases δ, although both V_{bi} and $V_{\text{bi}}^{\text{eff}}$ decrease due to V_f. The overall result is a significantly increased TE and, at the same time, a reduction of the TFE.

Considering the case in which the traps' profile consists of a continuous band of interfacial acceptorlike states with an energetic distribution, covering a wide range above and below E_F, then the states above E_F are not occupied, and thus they would not contribute at all to the current at the equilibrium condition. Similarly, although the acceptorlike states that lay below E_F are highly likely to be occupied, their effect would be an increment of the SBH [46], which, in turn, would further limit the already small percentage of electrons that were allowed to cross the barrier with TE from the tail of their occupation distribution. The large concentration of the occupied acceptorlike states would degenerate the initial metal/n-type 3C-SiC-on-Si with the emulated negative charge. Hence, although the barrier increases, this increment should feature a very thin triangular shape due to band bending. Therefore, the limited TE will be balanced by the TFE. Moreover, the recombination with TAT will not be favored due to the energetic positions of these states below the relative position of E_F at the Schottky interface. For these positions in the energy axes, the barrier separating the activated acceptorlike states and the occupation distribution is relatively thick. In consequence, both direct (FE) and indirect tunneling (TAT) would have a negligible contribution.

Fig. 4 illustrates a scenario where the interfacial traps' profile features a distribution of acceptorlike states closer to E_C and a distribution of donorlike states below E_0. At zero bias, the position of E_F at the interface, in this case, also determines a positive charge, however, less compared to the one formed in Fig. 3. In turn, the induced δ value and the amount of electrons able to transport with TFE will decrease.

Fig. 5 depicts the same traps distribution but at higher forward bias, while $V_f < V_{\text{bi}}$. The relative position of E_F at the Schottky interface moves upward, and under these conditions, the acceptorlike states energetically located below E_F can become occupied, i.e., forming a negative charge. $V_{\text{bi}}^{\text{eff}}$ becomes larger than V_{bi} near the interface, δ becomes negative, and the charge causes the bands to bend and to form a "thin triangular-shaped" region located at higher energies than the original barrier. In consequence, the effective barrier height increases. The contribution of TFE is sufficient through this

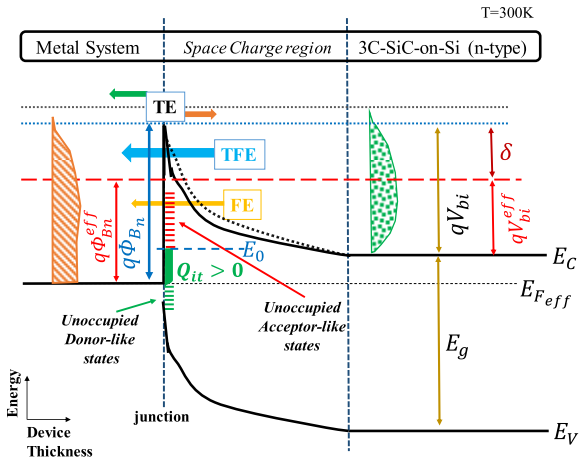

Fig. 4. At the metal/3C-SiC-on-Si interface, both donorlike and acceptorlike states exist separated by the notation of the neutrality level. In equilibrium, E_F determines a positive charge due to the donorlike states still energetically remaining above this level. The dotted E_C represents the initial bending due to the depletion region without any effect from interfacial states. Red states resemble acceptors and green resembles donor traps.

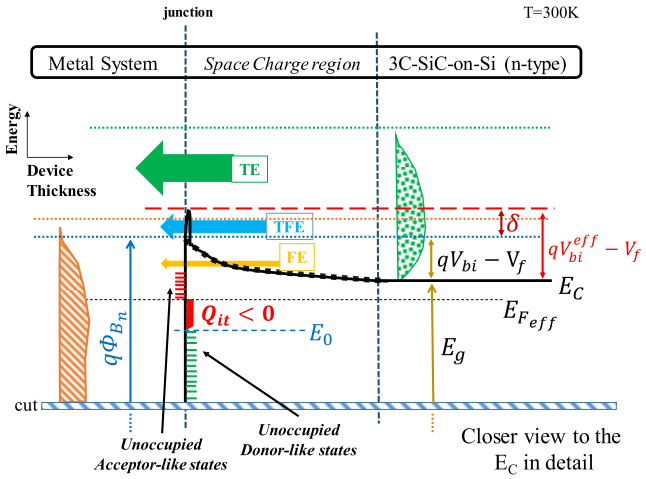

Fig. 5. At the metal/3C-SiC-on-Si interface, both donorlike and acceptorlike states exist separated by the notation of the neutrality level. The application of forward bias forces E_F to move upward. This alters the condition illustrated in Fig. 4 and acceptorlike traps now become ionized, thus highly likely to be occupied by an electron. This can balance the previously strong effect the charged donorlike states introduced to the barrier height.

thin region, although reduced compared to the previous bias condition in Fig. 4.

It is thus interesting to note the impact of bias condition on the effective built-in potential as described in Figs. 4 and 5 where the interfacial traps' profile features a distribution of acceptorlike states closer to E_C and a distribution of donorlike states below E_0. The type of charged states and their strength changes with bias that directly affects the TFE current element. The FEs in both these bias cases remain less important, whereas the TE eventually becomes the dominating factor but only when the bias approaches V_{bi}.

Moreover, the presence of states in all the aforementioned scenarios, i.e., in Figs. 3–5, can also stimulate TAT. The impact of forward bias on TAT is explained as follows. The Fermi level and the bands of the semiconductor move further up increasing their energy. Electrons tend to move from a

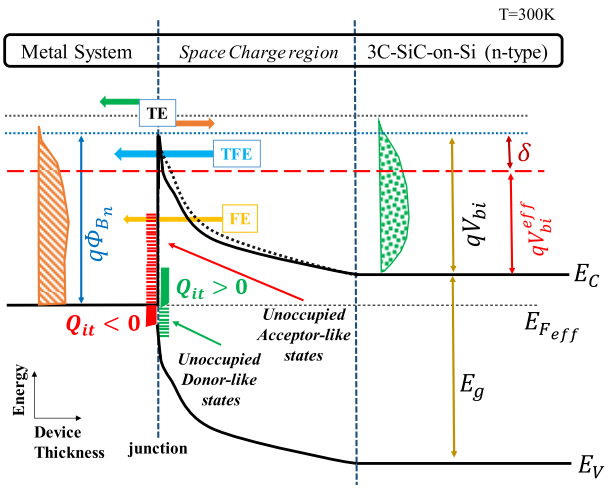

Fig. 6. Amphoteric interfacial traps at the metal/3C-SiC-on-Si increase the complexity of the modeled effect on the SBH, by counterbalancing their influence, but also offer more degrees of freedom in matching characterized diodes. The dotted E_C represents the initial bending due to the depletion region without any effect from interfacial states.

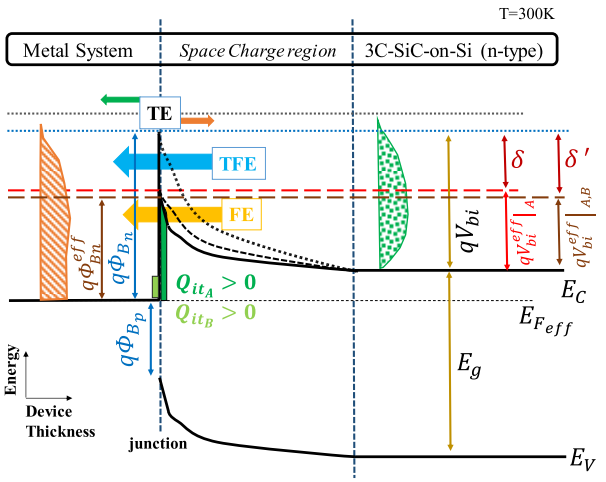

Fig. 7. Nonuniformities of the SBH resembled on the same band diagram. Two interfacial trap profiles, A and B, featuring different donorlike state distributions are able to model a first patch region (solid E_C). The dashed E_C corresponds to the effect induced considering only the trap profile A, which is a similar case to the one shown in Fig. 3 and can resemble a second patch. The dotted E_C represents a case without any effect from interfacial states.

higher E_F level to a lower E_F level side; thus, in these conditions, they favor a move from the semiconductor to the metal ($E_F^{3C-SiC} > E_F^{Metal}$). Donorlike interfacial states above E_F are able to release majority carriers to the metal side (capture a hole). Thus, electrons in the occupation distribution of the n-type 3C-SiC-on-Si conduction band that is energetically located lower than the formed V_{bi}^{eff} are now very likely to be captured from the ionized (occupied by holes) interfacial donor states, giving rise to TAT recombination. In addition, the donorlike states can become positively charged, as described earlier, and induce band bending that further encourages the TAT mechanism. Similarly, acceptorlike states below E_F absorb majority carriers in the vicinity of the interface from the semiconductor side. In this condition, they are able to capture holes from the metal side, i.e., resembling the completion of a TAT recombination process. However, the TAT recombination originating from acceptorlike states below the E_F can be less intense compared to an equivalent case with donorlike states above E_F. That is because tunneling in the latter takes place at a lower energy where a higher part of the occupation distribution meets the correct energy requirement.

Therefore, the donorlike interfacial states contribute to the current by enhancing both the TFE and the indirect TAT recombination, while the acceptorlike ones mainly affect the TAT recombination processes. In both cases, the resultant carriers' flow adds to the TE and shapes the subthreshold current of the power diode.

In the extreme case of the presence of amphoteric interfacial traps [47], [48], we have states at the same energy which can behave both as acceptors and donors. This is illustrated in Fig. 6. Depending on the forward bias level, positive charge, from the occupied donorlike states, is compensated by negative charge, originating from the occupied acceptorlike states. Accordingly, this can alter the contribution of the TFE, FE, and TAT recombination to the resultant current.

Summarizing, the exact I–V relationship and the amount of majority carriers flowing toward the metal side, while in the sub-threshold region at every bias condition, are directly affected by the exact interface traps' profile. We argue that a spatially uniform distribution of this traps' profile along all the Schottky contact essentially defines a uniform behavior of the SBH for this contact. Thereafter, this uniform behavior can be disrupted by the introduction of multiple additional trap profiles featuring different spatial properties along the Schottky contact.

B. Modeling the Nonuniformities of the Schottky Barrier Height

Nonuniformities of the SBH can be modeled by defining multiple interfacial trap profiles that must act in patches at different locations on the Schottky contact. This is illustrated in the same band diagram shown in Fig. 7. The solid line resembles what could be a "patch region one," while the dashed one resembles what could be a "patch region two." In "patch region two," the profile of the states can be similar to what is described in Fig. 3—for simplicity, we will refer to it as "profile A." In the "patch region one," there can exist "profile A" but also "profile B." The traps' "profile B" can introduce different states' distributions of a different neutrality level. In the scenario of Fig. 7, trap "profile B" consists of donorlike states close to E_C. Q_{itA} corresponds to the charged donorlike states from the "profile A." On the other hand, Q_{itB} corresponds to additional charged donorlike states contained in the "profile B," which is energetically expanding in a narrower band of energies. This emulates a lower SBH value on the Schottky contact for the "patch region one" compared to the "patch region two" in which only the trap "profile A" applies. As with previous cases, the application of bias strongly affects which one of those two trap profiles, and thus patches, will be more active. For $V_f \ll V_{bi}$,

in "patch region one," both donorlike state distributions form a positive charge, creating enhanced electric field conditions at the interface. In turn, the TFE, FE, and TAT recombination becomes more dominant compared to the rest of the contact area. Consequently, δ' becomes larger for "patch region one" ($\delta' > \delta$), indicating a smaller $V_{\text{bi}}^{\text{eff}}|_{A,B}$ and thus a smaller SBH value, as shown in Fig. 7. With the applied forward bias increasing, both Q_{itA} and Q_{itB} reduce. Beyond a specific bias level, E_F will eventually overcome the shallowest donorlike energy level of the interfacial trap "profile B" and Q_{itB} will become zero. Thereafter, only "profile A" will affect the carriers' transport, thus determining a larger effective build-in potential ($V_{\text{bi}}^{\text{eff}}|_A$). In turn, the TAT recombination will reduce, resulting in a different η value, closer to unity. In consequence, the subthreshold region of the $\log(I)$–V curve will feature two different slopes. Similarly, even more complex curves of the subthreshold current can be associated with the presence and contribution of even more complex states profiles and patches at the Schottky interface.

The spatial information of any additional traps' profile, which accounts for a localized nonuniformity of the SBH, remains arbitrary and can be adjusted given the actual states' distribution for each Schottky contact. Thus, it is assumed that any patch definition will expand within a particular percentage of the total Schottky contact area. Currently, it is not possible to determine the exact location and the dimensions of the patch, responsible for the inhomogeneity, within the Schottky active area. Given the accurate TCAD model of the diode and the utilization of the area factor, the percentage of the actual active area over which the additional trap-profile spatially expands should be decided with simulations.

III. Attributing the Subthreshold Current to the Interfacial States—Case Study

A. 3C-SiC-on-Si Schottky Barrier Diode TCAD Modeling Methodology

The vertical power SBD, considered in this article, features cylindrical contacts and its fabrication was reported in [42]. The Schottky interface was formed from the evaporation of platinum (Pt) on a 4-μm-thick nonfreestanding drift layer of the 3C-SiC material, epitaxially grown on Si. The area of the Schottky contact is smaller than that of the back titanium (Ti) ohmic one in order to deal with parasitic capacitance elements of the device [49]. Consequently, a fraction of 3C-SiC surface is exposed on the top. A buffer layer of 1 μm is included resulting in a punchthrough design. The Si substrate is approximately 500 μm thick [50], while all the layers are nitrogen (N) doped. The design details can be identified in the device cross-sectional view illustrated in Fig. 8.

The annealing process for contact smoothing eventually forms platinum silicides (PtSi) [46]. The work function of PtSi is still greater than the electron affinity of the n-doped cubic SiC ($\Phi_{\text{PtSi}} > X_{3C}$). This indicates that, after contact, majority electrons flow from the semiconductor to the metal to reach equilibrium. This flow lowers the potential energy of the bands at the 3C-SiC side. The SBH, or metal–semiconductor work function (Φ_{B_n}), formed governs the current transport in the SBD.

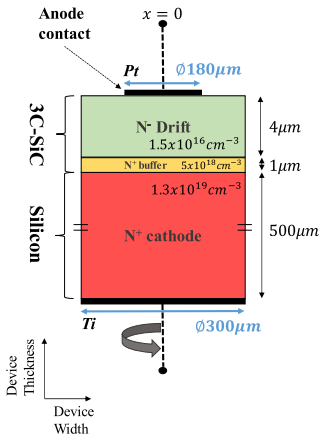

Fig. 8. TCAD simulated cylindrical asymmetric SBD structure based on an isotype 3C-SiC on Si heterointerface.

TABLE I
Basic Parameters of Bulk 3C-SiC for the Band Diagram

Parameter	Bulk 3C-SiC
Bandgap (E_g) at T=300K [eV]	2.353
Intrinsic carrier concentration (n_i) [cm^{-3}]	0.2285
Electron affinity [eV]	3.83

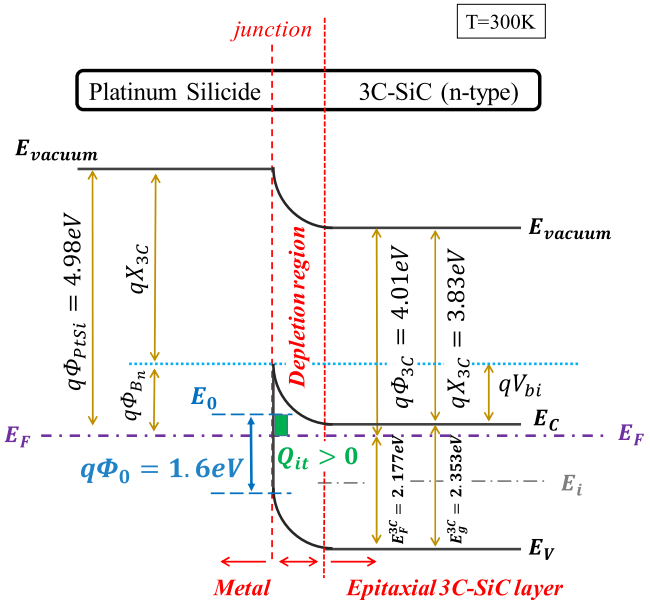

Fig. 9. Band diagram of the Schottky contact between n-type 3C-SiC-on-Si and thin PtSi. The interfacial traps' Profile A, in Table II, and the position of E_F decide the formed positive interface charge.

The band diagram of the investigated SBD is illustrated in Fig. 9. The work function of thin PtSi, $q\Phi_{\text{PtSi}} = 4.98$ eV [51] and the validated bulk 3C-SiC parameters [43], [52], listed in Table I, have been employed in the calculations. For the accurate representation of E_F in the bulk, the bandgap narrowing phenomenon has been considered in

the calculations in (1), where n_0 is the equilibrium concentration of majority electrons at $T = 300$K. The band diagram assists in identifying the relative position of E_F at the Schottky interface, which is crucial information for the discussed model.

$$n_0 = n_i \exp\left(\frac{E_F - E_g/2}{kT}\right). \quad (1)$$

B. Suggested Model on the Subthreshold Current Assuming a Spatially Uniform SBH Behavior

Synopsys Sentaurus Structure Editor [53] and Synopsys Sentaurus Device [54] were utilized to simulate the 2-D model of the SBD depicted in Fig. 8 with the application of a proper area factor value. The design methodology includes an initial simulation without the inclusion of any bulk or interfacial trap profiles in order to obtain the subthreshold current as predicted from the TE only. Thereafter, the comparison between the obtained $\log(I)$–V and the measurements assists in deciding which case of interfacial trap distributions, from the ones described in Section II, is more likely to cause the differentiations between the simulated and the observed current. The band diagram of the diode largely assists toward this direction because it contains critical information, i.e., the position of E_F. Utilizing the information of the relative position of E_F at the Schottky interface and the selected case of the traps' profile, the distribution properties of the donor and/or acceptorlike states within this trap profile are roughly estimated. The mean and sigma values of these Gaussian distributions are set in such a way so that the neutrality level can be determined. Thus, E_0 is not defined in the simulations, rather it arises as the energy level that separates the two Gaussian distributions of the interfacial traps' profile. Finally, the concentration and the exact range of energies for each state type are identified through extensive simulations and comparison to the experimental results.

According to the suggested model in this article, a trap profile is considered, featuring states with a continuous band of energies at the PtSi/3C-SiC-on-Si interface. Focusing on the subthreshold current measurements of the investigated diode, subsequent TCAD simulations were carried out to identify the distributions of these interfacial states. The best match between measurements and simulations was obtained with the introduction of a traps' profile with both donorlike and acceptorlike distributions (Profile A), resembling the case illustrated in Fig. 4, and properties as listed in Table II. The result, which compares the measurements with the simulations considering uniform SBH behavior, is shown at the end of this section.

The simulations revealed that E_0, separating the two distributions of the traps' Profile A, should be energetically considered above E_F in equilibrium, as illustrated in Fig. 10. The notation Φ_0 is used to identify the neutrality level with respect to the valence band (E_V). This implies that a positive charge is formed at the Schottky interface due to occupied interfacial donorlike deep levels, as shown in Fig. 9.

The characterized states, in Profile A, are coupled with the Schottky contact through a calibrated nonlocal TAT

TABLE II
IDENTIFIED DEFECTS IN THE INVESTIGATED 3C-SIC-ON-SI SBD

Traps' Description	Type	Concentration	Energetic Distribution
Schottky interfacial states resulting in a specific effect on the SBH **(Profile A)**	Donor	$6\text{x}10^{12}\,cm^{-2}$	Gaussian $E_{Mid}^{from\,E_V} = 0.8eV$, $E_{Sig} = 0.8eV$
	Acceptor	$5\text{x}10^{12}\,cm^{-2}$	Gaussian $E_{Mid}^{from\,E_C} = 0.4eV$, $E_{Sig} = 0.4eV$
Bulk deep levels due to 3C-SiC/Si hetero-interface	Acceptor	$1.5\text{x}10^{16}\,cm^{-3}$	Single Level Activation Energy [55]: $E^{from\,E_V} = 0.5eV$

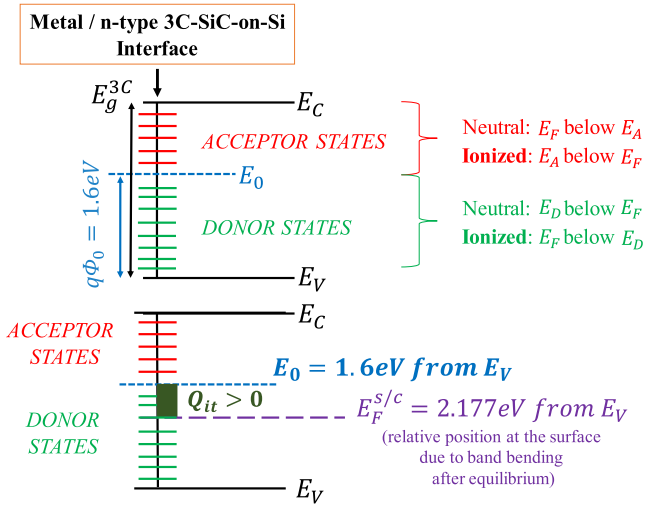

Fig. 10. Continuous band of donor and acceptor states in conjunction with the assumed position of E_0 and the calculated position of E_F for the n-type 3C-SiC-on-Si produces a positive charge at the Schottky interface while in equilibrium. The energies of the acceptor and donor states are indicated as E_A and E_D correspondingly.

TABLE III
MOBILITY AND TUNNELING PARAMETERS

Parameter	3C-SiC	
	electrons	holes
Mobility [cm^2/Vs]	650	50
Tunnelling mass [in units of m_0]	0.05	0.05
Interface prefactor (g_C)	$1\text{x}10^{-3}$	$0.66\text{x}10^{-2}$

model [56]. The values of the parameters for this model were fine-tuned for 3C-SiC, as shown in Table III, to achieve the best match to the experimental data [42]. The tunneling mass of electrons is a dimensionless property of the material that forms the tunneling barrier, whereas the prefactor (g_C) refers to the ratio between the effective [57] and the free electrons Richardson constant [58].

Furthermore, to accurately emulate the ON-state performance, the influence of bulk acceptor traps was also required

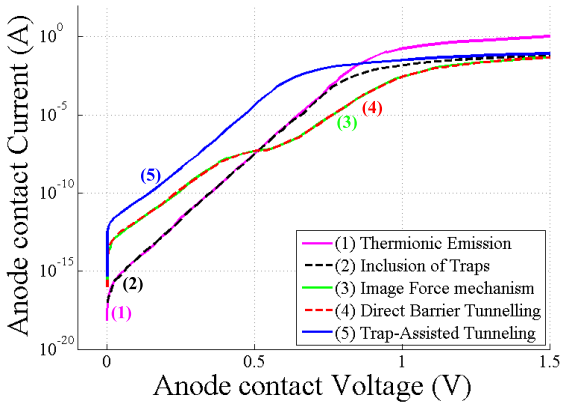

Fig. 11. Combined contribution of the identified traps in Table II and their effect on the majority carriers' transport after TCAD simulations of the investigated 3C-SiC-on-Si SBD.

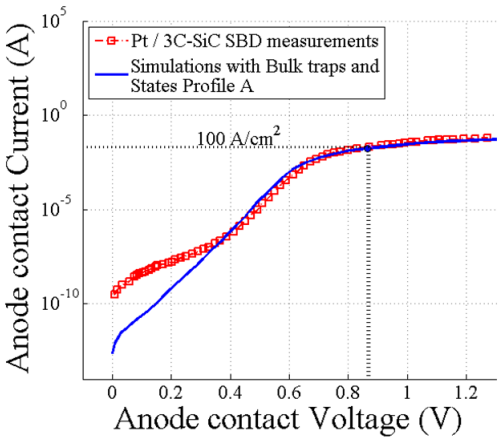

Fig. 12. TCAD simulated log(I)–V characteristics of the investigated Pt/3C-SiC-on-Si SBD after the inclusion of the traps in Table II is in a very good agreement to the experimental data [42].

in the simulations. These deep levels, originating from the 3C-SiC/Si heterojunction region, are modeled to spatially distribute in a uniform manner throughout the 3C-SiC epilayer. The properties of the bulk traps are given in Table II. Such bulk traps affect the majority carriers' transport by capturing and releasing electrons, which decreases their mobility and, in turn, increases the simulated on-resistance. The defects generated at the heterointerface of 3C-SiC to Si are mainly attributed to the out-diffusion of Si from the substrate in order to contribute to the formation of the overlying SiC layer [15]. To the credit of this article, the TCAD simulation results are in line with reported observations for the 3C-SiC, which consider the silicon vacancy (V_{Si}) to act as a deep acceptor level [59]. Moreover, the observed simulated behavior of the introduced deep levels originating from the 3C-SiC/Si heterointerface resembles the presence of stacking faults (SFs). The SFs in 3C-SiC are highly electrically active also causing scattering of electrons especially in n-type materials [60]. This source of increased resistivity is the main cause of power device degradation. More specifically, the accumulated N at such crystallographic defects creates preferable paths for the current to flow in 3C-SiC [61].

All the identified defects (interfacial traps' Profile A and bulk traps) affect the carrier transport and accordingly the shape of the SBD log(I)–V curve. Simulation results shown in Fig. 11 give an insight into how the presence of these defects impacts the current mechanisms, which are subsequently activated. In particular, in curve 1, only the TE is activated in the simulations of the power device. In curve 2, the inclusion of the interfacial traps' Profile A does not have a strong contribution in the subthreshold current unless additional interacting mechanisms are involved to describe its effect on the SBH. The deep level bulk acceptor traps mainly affect the postthreshold part of the I–V characteristic by draining majority carriers and, thus, limiting the ON-state current level. In curve 3, the image force lowering, due to the depletion region charge and the charged donorlike interface states, signifies the contribution of the TFE current. This results in more carriers crossing the barrier for the same potential energy and temperature. In curve 4, the barrier tunneling mechanism is activated to account for the FE of electrons. Finally, in curve 5, the calibrated nonlocal TAT model accommodates for the indirect tunneling of electrons through the identified interfacial states of Profile A.

Interestingly, the simulations in Fig. 11 indicate an almost negligible contribution of the FE mechanism to the subthreshold current. In fact, the specification of the interfacial states' distributions is responsible for this behavior. The positive charge formed due to the portion of the donorlike states that become occupied is relatively small. Thus, the resultant band bending induced by this charge is not significant and the barrier shape does not get thin enough to strengthen the FE of the majority carriers. At the same time, the occurred band bending encourages TAT by moving the occupation distribution of electrons closer to the interfacial states. If the distribution of the interfacial states featured only donorlike traps as shown in Fig. 3, then the FE element of the total current would be greater at the expense of the TAT element. Comparing curve 1, in Fig. 11, to the final simulated forward bias log(I)–V curve of the SBD in Fig. 12, it is clear that the subthreshold current is a representative indicator of the semiconductor material quality in 3C-SiC-on-Si.

The proposed TCAD model, with the inclusion of the identified defects in Table II, is able to replicate accurately both the forward and reverse electrical performances of the SBD. A very good match between the simulations and the measurements is obtained, as shown in Figs. 12 and 13.

Notably, the effect of the interfacial traps' Profile A, in Table II, suggests a specific behavior of the SBH. Although this simulated behavior is in agreement with the forward experimental data, it is still weak in accurately predicting the subthreshold current for early forward bias conditions, as shown in Fig. 12.

C. Expanding the Suggested Model to Accommodate for the Inhomogeneous Features of the Investigated Schottky Contact

It is reasonable to argue that the Schottky interface in SiC would not feature uniform properties in the lateral direc-

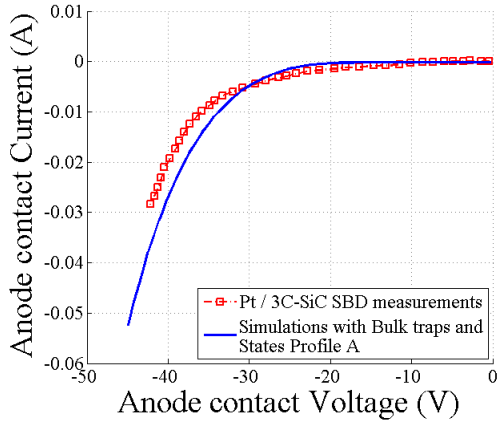

Fig. 13. Reverse characteristics can also be accurately predicted with the inclusion of the traps in Table II.

tion [20], [62]–[66]. In the case of the investigated SBD, the small mismatch observed in the early forward bias stages in Fig. 12 can be attributed to such an SBH inhomogeneity.

To model this in the simulations, a patch region on the Schottky contact is assumed to feature a second profile of interfacial states, additive to the existing Profile A. Within this small part of the contact, the added profile should consist of a donorlike states' distribution energetically located above the relative position of E_F at the Schottky interface. This will directly link their impact only to a limited set of early forward bias values; this corresponds to the simulated forward bias $\log(I)$–V region featuring the mismatch with the measurements. The concentration of these added donorlike states should be higher than the one defined in the previously identified Profile A, in order to ensure an elevated subthreshold current. As long as E_F is below these states, the likelihood of their switching between the unoccupied and the charged state is high. Furthermore, energetically above these extra donorlike states, an additional acceptors' distribution succeeds, also with a higher concentration compared to the corresponding one in Profile A. This will balance the subthreshold current, after a specific value of the forward bias, by locally increasing the resistance. Thus, a tradeoff is formed between these two new concentration values. These additional interfacial distributions of states are grouped together, in Table IV, as Profile B, and their properties were determined through simulations. The patch region, where both traps' Profiles A and B apply, gives accurate result when it covers 30% of the total Schottky contact. Essentially, this patch region describes the nonuniformity of the SBH. The addition of the interfacial traps' Profile B in the TCAD model and its supplementary effect on the electrons' transport mechanisms results in simulations that can accurately predict the subthreshold and the ON-state electrical performance. This is shown in Fig. 14.

Moreover, as shown in Fig. 15, the assumed patch region on the simulated Schottky contact does not influence the very good prediction of the reverse performance, obtained previously in Fig. 13. In reverse bias, the main contribution on the current is due to TAT generation processes through the ionized donorlike states. With the increased reverse bias,

TABLE IV
ADDITIONAL INTERFACIAL TRAP PROFILE TO MODEL THE SBH INHOMOGENEITY

Traps' Description	Type	Concentration	Distributions	
			Energetic	Spatial
Schottky interfacial states to model a Non-Uniform SBH value **(Profile B)**	Donor	$4\text{x}10^{19}\ cm^{-3}$	Gaussian $E_{Mid}^{from\ E_V} = 1eV$ $E_{Sig} = 0.3eV$	Covering 30% of the Schottky contact in the «Device Width» axis
	Acceptor	$2\text{x}10^{18}\ cm^{-3}$	Gaussian $E_{Mid}^{from\ E_V} = 1.7eV$ $E_{Sig} = 0.4eV$	

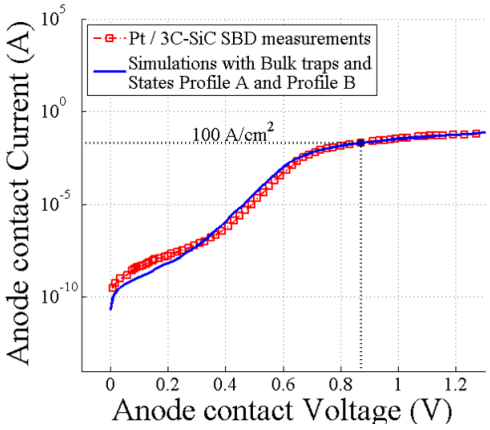

Fig. 14. Inclusion of the interfacial states' Profile B, which acts as additive to the states' Profile A, makes the suggested TCAD model able to predict the observed non-uniformity of the SBH in the lowest part of the measured $\log(I)$–V characteristics of the SBD [42]. The traps' Profile B is described in Table IV.

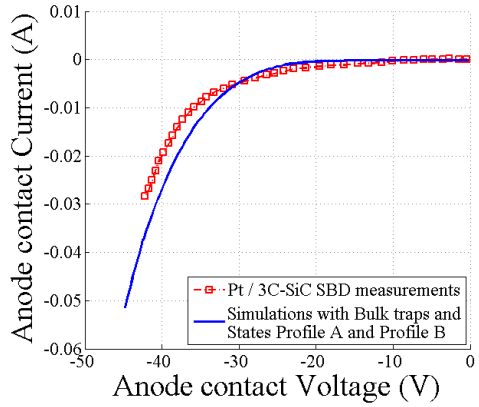

Fig. 15. Inclusion of the additional interfacial states' Profile B in Table IV does not disrupt the donorlike state distribution below E_F, as defined in the traps' Profile A in Table II, thus the generation current in reverse bias will remain mainly unaltered.

the relative position of E_F in Fig. 10 will energetically drop lower for all the Schottky contact, and more interfacial donorlike states will become occupied by a hole. Furthermore, the electrons will now favor a move from the metal side to the semiconductor side ($E_F^{\text{Metal}} > E_F^{\text{3C-SiC}}$). The generation process is then realized with these occupied states, first, emitting the captured hole to E_V^{Metal} and then emitting the trapped electron to $E_C^{\text{3C-SiC}}$. This two-step process depends

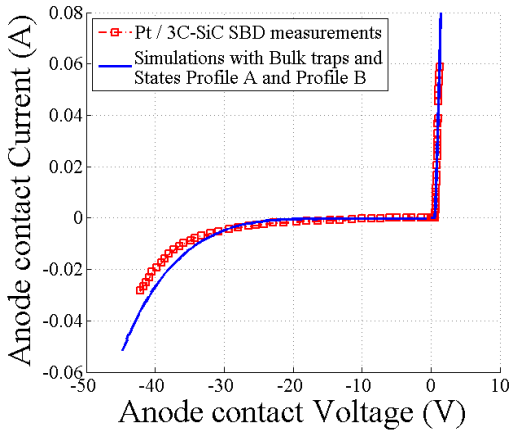

Fig. 16. Predicted I–V from the proposed model in this article, and the measurements [42] indicate that the identified defects accurately describe the net electrical performance of the diode.

on the concentration of the interfacial donorlike states that were energetically located below E_F in equilibrium. The specifications of the additional trap Profile B, in Table IV, will not entail any change to the concentration of these traps; therefore, Figs. 13 and 15 are almost identical.

When all the identified defects, as described in Tables II and IV, are included in the TCAD model, the simulation results are in excellent agreement with the measurements regarding both the forward (subthreshold, ON-state) and reverse bias conditions. Comprehensively, the final matching is also illustrated in Fig. 16 in the linear scale.

IV. Conclusion

In this article, the development of a highly accurate and deeply physical model is proposed to describe the nonideal behavior of the SBH in SBDs due to the presence of defects. To validate the model, the experimental performance of a fabricated 3C-SiC-on-Si SBD is used. Various combinations and cases of traps were regarded and their subsequent effects on the carrier transport mechanisms were thoroughly presented, analyzed, and illustrated. As the subthreshold region of the $\log(I)$–V measurements carries considerable information relevant to these defects, it is exploited in identifying their properties. According to the proposed model, an interfacial traps' profile is initially considered by modeling both donorlike and acceptorlike states. Each state type features its own energetic distribution and concentration. It has been shown that the specifications of a single interfacial traps' profile, spatially expanding over the total active area, determines a certain SBH behavior owned to the effect of these traps on the carrier transport mechanisms. By modeling the additional traps profiles that are spatially present over parts of the Schottky interface, it has been achieved, for the first time, to model the observed inhomogeneity of the SBH and to explain the physics behind it. In consequence, the suggested model is able to sufficiently predict complex subthreshold leakage current—voltage relationships by appropriately characterizing these trap profiles. This can be considered as an advantage over Tung's model, which can also be utilized to describe nonuniform Schottky contacts, but its application is delimited by the ideality factor value of the diode.

The way the determined defects affect the carrier transport mechanisms has also been analyzed, with the role of the Schottky interfacial states on the TAT generation and recombination current revealed to depend on the bias condition. Since both the subthreshold and the leakage current of the SBD can be accurately described and explained by the model, the quality of the Schottky contact (in terms of the presence of states) can be evaluated and understood. The ON-state has been found to be mainly affected by bulk deep levels. In this article, these deep levels have been characterized as V_{Si} acceptor type in the 3C-SiC epilayer. These defects are due to the out-diffusion of Si originating from the heterointerface between the 3C-SiC and the substrate. Finally, potential similarities of the modeled bulk traps to the reported electrical behavior of SFs in 3C-SiC are encouraging and require further investigation.

In conclusion, the TCAD model, with the inclusion of the identified interfacial trap profiles and bulk deep levels, allowed for an excellent prediction of the total electrical performance of the investigated 3C-SiC-on-Si SBD. Indeed, the simulation results, presented in this article, are in excellent agreement with the measurements for both the forward bias and the reverse bias. The ability to analyze and model such complex behavior enables the optimization of fabrication strategies that would allow the reduction/elimination of interfacial states but also the design of device structures, which could mitigate from those. Finally, it should be highlighted that the suggested model is not limited only to 3C-SiC-on-Si substrate diodes rather it can be applied to any SBD, enabling for the identification of the defects (both Schottky interface states and bulk traps) and their subsequent effect on the electrical performance of the power diode. To also highlight the ability of the model to work when strong nonidealities exist and to provide the relevant physical insight of the underlying causes of those, where other models, e.g., Tung's model, do not work.

References

[1] X. She, A. Q. Huang, Ó. Lucía, and B. Ozpineci, "Review of silicon carbide power devices and their applications," *IEEE Trans. Ind. Electron.*, vol. 64, no. 10, pp. 8193–8205, Oct. 2017. doi: 10.1109/TIE.2017.2652401.

[2] Y. K. Sharma, "Introductory chapter: Need of SiC devices in power electronics—A beginning of new era in power industry," in *Disruptive Wide Bandgap Semiconductors, Related Technologies, and Their Applications*, Y. K. Sharma, Ed. Rijeka, Croatia: InTech, 2018, pp. 1–16.

[3] H. Morkoç, S. Strite, G. B. Gao, M. E. Lin, B. Sverdlov, and M. Burns, "Large-band-gap SiC, III-V nitride, and II-VI ZnSe-based semiconductor device technologies," *J. Appl. Phys.*, vol. 76, no. 3, pp. 1363–1398, 1994. doi: 10.1063/1.358463.

[4] F. Ciobanu *et al.*, "Traps at the interface of 3C-SiC/SiO_2-MOS-structures," *Mater. Sci. Forum*, vols. 433–436, pp. 551–554, Sep. 2003. doi: 10.4028/www.scientific.net/MSF.433-436.551.

[5] A. A. Lebedev, S. P. Lebedev, V. Y. Davydov, S. N. Novikov, and Y. N. Makarov, "Growth and investigation SiC based heterostructures," in *Proc. 15th Biennial Baltic Electron. Conf. (BEC)*, Oct. 2016, pp. 4–5. doi: 10.1109/BEC.2016.7743717.

[6] M. Krieger, G. Pensl, M. Bakowski, H. Nagasawa, M. Abe, and A. Schöner, "Hall effect in the channel of 3C-SiC MOSFETs," *Mater. Sci. Forum*, vol. 485, pp. 441–444, May 2005. doi: 10.4028/www.scientific.net/MSF.483-485.441.

[7] K. K. Lee *et al.*, "N-channel MOSFETs fabricated on homoepitaxy-grown 3C-SiC films," *IEEE Electron Device Lett.*, vol. 24, no. 7, pp. 466–468, Jul. 2003.

[8] T. Ohshima *et al.*, "The electrical characteristics of metal-oxide-semiconductor field effect transistors fabricated on cubic silicon carbide," *Jpn. J. Appl. Phys.*, vol. 42, p. L625, Jun. 2003. doi: 10.1143/JJAP.42.L625.

[9] G. Ferro, "3C-SiC heteroepitaxial growth on silicon: The quest for holy grail," *Crit. Rev. Solid State Mater. Sci.*, vol. 40, no. 1, pp. 56–76, 2015. doi: 10.1080/10408436.2014.940440.

[10] F. Roccaforte, F. Giannazzo, and V. Raineri, "Nanoscale transport properties at silicon carbide interfaces," *J. Appl. Phys.*, vol. 43, no. 22, May 2011, Art. no. 223001.

[11] P. Hens, G. Wagner, A. Hölzing, R. Hock, and P. Wellmann, "Dependence of the seed layer quality on different temperature ramp-up conditions for 3C-SiC hetero-epitaxy on Si (100)," *Thin Solid Films*, vol. 522, pp. 2–6, Nov. 2012. doi: 10.1016/j.tsf.2011.10.177.

[12] A. Stefanskyi, L. Starzak, and A. Napieralski, "Silicon carbide power electronics for electric vehicles," in *Proc. 10th Int. Conf. Ecol. Veh. Renew. Energies*, Mar./Apr. 2015, pp. 1–9. doi: 10.1109/EVER.2015.7138047.

[13] G. Colston *et al.*, "Mapping the strain and tilt of a suspended 3C-SiC membrane through micro X-ray diffraction," *Mater. Des.*, vol. 103, pp. 244–248, Aug. 2016. doi: 10.1016/j.matdes.2016.04.078.

[14] Y. Li *et al.*, "Heteroepitaxial 3C-SiC on Si (100) with flow-modulated carbonization process conditions," *J. Cryst. Growth*, vol. 506, pp. 114–116, Jan. 2019. doi: 10.1016/j.jcrysgro.2018.09.037.

[15] F. La Via *et al.*, "From thin film to bulk 3C-SiC growth: Understanding the mechanism of defects reduction," *Mater. Sci. Semicond. Process.*, vol. 78, pp. 57–68, May 2018. doi: 10.1016/j.mssp.2017.12.012.

[16] H. Nagasawa, K. Yagi, T. Kawahara, and N. Hatta, "Reducing planar defects in 3C–SiC," *Chem. Vapor Deposition*, vol. 12, nos. 8–9, pp. 502–508, 2006. doi: 10.1002/cvde.200506466.

[17] D. Chaussende *et al.*, "Prospects for 3C-SiC bulk crystal growth," *J. Cryst. Growth*, vol. 310, no. 5, pp. 976–981, Mar. 2008. doi: 10.1016/j.jcrysgro.2007.11.140.

[18] R. Anzalone *et al.*, "Growth rate effect on 3C-SiC film residual stress on (100) Si substrates," *Mater. Sci. Forum*, vols. 645–648, pp. 143–146, Apr. 2010. doi: 10.4028/www.scientific.net/MSF.645-648.143.

[19] J. Eriksson, M. H. Weng, F. Roccaforte, F. Giannazzo, S. Leone, and V. Raineri, "Toward an ideal Schottky barrier on 3*C*-SiC," *Appl. Phys. Lett.*, vol. 95, no. 8, 2009, Art. no. 081907. doi: 10.1063/1.3211965.

[20] S. Roy, C. Jacob, and S. Basu, "Current transport properties of Pd/3C–SiC Schottky junctions with planar and vertical structures," *Solid State Sci.*, vol. 6, no. 4, pp. 377–382, Apr. 2004. doi: 10.1016/j.solidstatesciences.2004.01.003.

[21] J. Komiyama, Y. Abe, S. Suzuki, T. Kita, and H. Nakanishi, "Schottky diode characteristics of 3C-SiC grown on a Si substrate by vapor phase epitaxy," *J. Cryst. Growth*, vol. 275, nos. 1–2, pp. 1001–1006, 2005. doi: 10.1016/j.jcrysgro.2004.11.155.

[22] D. K. Schroder, "Carrier lifetimes in silicon," *IEEE Trans. Electron Devices*, vol. 44, no. 1, pp. 160–170, Jan. 1997.

[23] W. Monch, "On the physics of metal-semiconductor interfaces," *Reports Prog. Phys.*, vol. 53, no. 3, pp. 221–278, Mar. 1990. doi: 10.1088/0034-4885/53/3/001.

[24] R. T. Tung, "The physics and chemistry of the Schottky barrier height," *Appl. Phys. Rev.*, vol. 1, no. 1, 2014, Art. no. 011304. doi: 10.1063/1.4858400.

[25] R. T. Tung, "Electron transport at metal-semiconductor interfaces: General theory," *Phys. Rev. B, Condens. Matter*, vol. 45, no. 23, pp. 13509–13523, Jun. 1992. doi: 10.1103/PhysRevB.45.13509.

[26] V. Kumar, A. S. Maan, and J. Akhtar, "Barrier height inhomogeneities induced anomaly in thermal sensitivity of Ni/4H-SiC Schottky diode temperature sensor," *J. Vac. Sci. Technol. B, Microelectron.*, vol. 32, no. 4, 2014, Art. no. 041203. doi: 10.1116/1.4884756.

[27] M. E. Aydın, N. Yıldırım, and A. Türüt, "Temperature-dependent behavior of Ni/4H-*n*SiC Schottky contacts," *J. Appl. Phys.*, vol. 102, no. 4, 2007, Art. no. 043701. doi: 10.1063/1.2769284.

[28] G. S. Chung, K. S. Kim, and F. Yakuphanoglu, "Electrical characterization of Au/3C-SiC/n-Si/Al Schottky junction," *J. Alloys Compound*, vol. 507, no. 2, pp. 508–512, 2010. doi: 10.1016/j.jallcom.2010.08.004.

[29] J. H. Werner and H. H. Güttler, "Barrier inhomogeneities at Schottky contacts," *J. Appl. Phys.*, vol. 69, no. 3, pp. 1522–1533, Jan. 1991. doi: 10.1063/1.347243.

[30] S. U. Omar, T. S. Sudarshan, T. A. Rana, H. Song, and M. V. S. Chandrashekhar, "Large barrier, highly uniform and reproducible Ni-Si/4H-SiC forward Schottky diode characteristics: Testing the limits of Tung's model," *J. Phys. D. Appl. Phys.*, vol. 47, no. 29, 2014, Art. no. 295102. doi: 10.1088/0022-3727/47/29/295102.

[31] J.-L. Li *et al.*, "Influence of deep defects on electrical properties of Ni/4H-SiC Schottky diode," *Chin. Phys. B*, vol. 28, no. 2, 2019, Art. no. 027303. doi: 10.1088/1674-1056/28/2/027303.

[32] J. P. Sullivan, R. T. Tung, M. R. Pinto, and W. R. Graham, "Electron transport of inhomogeneous Schottky barriers: A numerical study," *J. Appl. Phys.*, vol. 70, no. 12, pp. 7403–7424, 1991. doi: 10.1063/1.349737.

[33] P. M. Gammon *et al.*, "Modelling the inhomogeneous SiC Schottky interface," *J. Appl. Phys.*, vol. 114, no. 22, 2013, Art. no. 223704. doi: 10.1063/1.4842096.

[34] F. La Via, M. Camarda, and A. La Magna, "Mechanisms of growth and defect properties of epitaxial SiC," *Appl. Phys. Rev.*, vol. 1, no. 3, 2014, Art. no. 031301. doi: 10.1063/1.4890974.

[35] Y. Yamamoto *et al.*, "Low-dislocation-density 4H-SiC crystal growth utilizing dislocation conversion during solution method," *Appl. Phys. Express*, vol. 7, no. 6, 2014, Art. no. 065501. doi: 10.7567/APEX.7.065501.

[36] M. Benamara, M. Anani, B. Akkal, and Z. Benamara, "Ni/SiC–6H Schottky barrier diode interfacial states characterization related to temperature," *J. Alloys Compounds*, vol. 603, pp. 197–201, Aug. 2014. doi: 10.1016/j.jallcom.2014.02.177.

[37] K.-Y. Lee and Y.-H. Huang, "An investigation on barrier inhomogeneities of 4H-SiC Schottky barrier diodes induced by surface morphology and traps," *IEEE Trans. Electron Devices*, vol. 59, no. 3, pp. 694–699, Mar. 2012. doi: 10.1109/TED.2011.2181391.

[38] T. Katsuno *et al.*, "Analysis of surface morphology at leakage current sources of 4H–SiC Schottky barrier diodes," *Appl. Phys. Lett.*, vol. 98, no. 22, 2011, Art. no. 222111. doi: 10.1063/1.3597413.

[39] K.-Y. Lee and M. A. Capano, "The correlation of surface defects and reverse breakdown of 4H-SiC Schottky barrier diodes," *J. Electron. Mater.*, vol. 36, no. 4, pp. 272–276, 2007. doi: 10.1007/s11664-006-0075-3.

[40] D. J. Ewing *et al.*, "Inhomogeneities in Ni/4H-SiC Schottky barriers: Localized Fermi-level pinning by defect states," *J. Appl. Phys.*, vol. 101, no. 11, 2007, Art. no. 114514. doi: 10.1063/1.2745436.

[41] K. C. Mandal, S. K. Chaudhuri, K. V. Nguyen, and M. A. Mannan, "Correlation of deep levels with detector performance in 4H-SiC epitaxial Schottky barrier alpha detectors," *IEEE Trans. Nucl. Sci.*, vol. 61, no. 4, pp. 2338–2344, Aug. 2014. doi: 10.1109/TNS.2014.2335736.

[42] P. Shenoy, A. Moki, B. J. Baliga, D. Alok, K. Wongchotigul, and M. Spencer, "Vertical Schottky barrier diodes on 3C-SiC grown on Si," in *IEDM Tech. Dig.*, Dec. 1994, pp. 411–414. doi: 10.1109/IEDM.1994.383380.

[43] A. Arvanitopoulos, N. Lophitis, K. N. Gyftakis, S. Perkins, and M. Antoniou, "Validated physical models and parameters of bulk 3C–SiC aiming for credible technology computer aided design (TCAD) simulation," *Semicond. Sci. Technol.*, vol. 32, no. 10, 2017, Art. no. 104009. doi: 10.1088/1361-6641/aa856b.

[44] M. Mandurrino *et al.*, "Trap-assisted tunneling in InGaN/GaN LEDs: Experiments and physics-based simulation," in *Proc. Int. Conf. Numer. Simulation Optoelectron. Devices (NUSOD)*, Sep. 2014, pp. 13–14. doi: 10.1109/NUSOD.2014.6935332.

[45] B. Asllani, M. Berthou, D. Tournier, P. Brosselard, and P. Godignon, "Modeling of inhomogeneous 4H-SiC Schottky and JBS diodes in a wide temperature range," *Mater. Sci. Forum*, vol. 858, pp. 741–744, May 2016.

[46] B. J. Baliga, *Fundamentals of Power Semiconductor Devices*. New York, NY, USA: Springer, 2008.

[47] M. Walters and A. Reisman, "Radiation-induced neutral electron trap generation in electrically biased insulated gate field effect transistor gate insulators," *J. Electrochem. Soc.*, vol. 138, no. 9, p. 2756, 1991. doi: 10.1149/1.2086050.

[48] F. Jazaeri, C.-M. Zhang, A. Pezzotta, and C. Enz, "Charge-based modeling of radiation damage in symmetric double-gate MOSFETs," *IEEE J. Electron Devices Soc.*, vol. 6, pp. 85–94, Nov. 2018. doi: 10.1109/JEDS.2017.2772346.

[49] D. K. Schroder, *Semiconductor Material and Device Characterization*, 3rd ed. New York, NY, USA: Wiley, 2006.

[50] C. M. Su, M. Wuttig, A. Fekade, and M. Spencer, "Elastic and anelastic properties of chemical vapor deposited epitaxial 3C-SiC," *J. Appl. Phys.*, vol. 77, no. 11, pp. 5611–5615, 1995. doi: 10.1063/1.359551.

[51] T. J. Drummond, "Work functions of the transition metals and metal silicides," Sandia Nat. Labs, Albuquerque, NM, USA, Tech. Rep. SAND99-0391J, 1999.

[52] N. Lophitis, A. Arvanitopoulos, S. Perkins, and M. Antoniou, "TCAD device modelling and simulation of wide bandgap power semiconductors," in *Disruptive Wide Bandgap Semiconductors, Related Technologies, and Their Applications*, Y. K. Sharma, Ed. Rijeka, Croatia: InTech, 2018.
[53] "Sentaurus TM structure editor user guide," Synopsys, Mountain View, CA, USA, 2017.
[54] "Sentaurus TM device user guide," Synopsys, Mountain View, CA, USA, 2017.
[55] H. Itoh *et al.*, "Intrinsic defects in cubic silicon carbide," *Phys. Status Solidi*, vol. 162, no. 1, pp. 173–198, 1997.
[56] A. Schenk, "A model for the field and temperature dependence of shockley-read-hall lifetimes in silicon," *Solid-State Electron.*, vol. 35, no. 11, pp. 1585–1596, 1992. doi: 10.1016/0038-1101(92)90184-E.
[57] N. Tōyama, "Effective Richardson constant of sputtered Pt-Si Schottky contacts," *J. Appl. Phys.*, vol. 64, no. 5, p. 2515, 1988. doi: 10.1063/1.341634.
[58] V. Saxena, J. N. Su, and A. J. Steckl, "High-voltage Ni- and Pt-SiC Schottky diodes utilizing metal field plate termination," *IEEE Trans. Electron Devices*, vol. 46, no. 3, pp. 456–464, Mar. 1999.
[59] L. Wenchang, Z. Kaiming, and X. Xide, "An electronic structure study of single native defects in beta-SiC," *J. Phys., Condens. Matter*, vol. 5, no. 7, pp. 891–898, Feb. 1993. doi: 10.1088/0953-8984/5/7/016.
[60] I. Deretzis, M. Camarda, F. La Via, and A. La Magna, "Electron backscattering from stacking faults in SiC by means of *ab initio* quantum transport calculations," *Phys. Rev. B, Condens. Matter*, vol. 85, no. 23, 2012, Art. no. 235310. doi: 10.1103/PhysRevB.85.235310.
[61] X. Song *et al.*, "Evidence of electrical activity of extended defects in 3C–SiC grown on Si," *Appl. Phys. Lett.*, vol. 96, no. 14, 2010, Art. no. 142104. doi: 10.1063/1.3383233.
[62] G. Pristavu, G. Brezeanu, M. Badila, R. Pascu, M. Danila, and P. Godignon, "A model to non-uniform Ni Schottky contact on SiC annealed at elevated temperatures," *Appl. Phys. Lett.*, vol. 106, no. 26, 2015, Art. no. 261605. doi: 10.1063/1.4923468.
[63] A. F. Hamida, Z. Ouennoughi, A. Sellai, R. Weiss, and H. Ryssel, "Barrier inhomogeneities of tungsten Schottky diodes on 4H-SiC," *Semicond. Sci. Technol.*, vol. 23, no. 4, 2008, Art. no. 045005. doi: 10.1088/0268-1242/23/4/045005.
[64] L. Boussouar, Z. Ouennoughi, N. Rouag, A. Sellai, R. Weiss, and H. Ryssel, "Investigation of barrier inhomogeneities in Mo/4H–SiC Schottky diodes," *Microelectron. Eng.*, vol. 88, no. 6, pp. 969–975, Jun. 2011. doi: 10.1016/j.mee.2010.12.070.
[65] S. Kyoung, E.-S. Jung, and M. Y. Sung, "Post-annealing processes to improve inhomogeneity of Schottky barrier height in Ti/Al 4H-SiC Schottky barrier diode," *Microelectron. Eng.*, vol. 154, pp. 69–73, Mar. 2016. doi: 10.1016/j.mee.2016.01.013.
[66] F. Giannazzo, F. Roccaforte, S. F. Liotta, and V. Raineri, "Two dimensional imaging of the laterally inhomogeneous Au/4H-SiC Schottky barrier by conductive atomic force microscopy," *Mater. Sci. Forum*, vols. 556–557, pp. 545–548, Sep. 2007. doi: 10.4028/www.scientific.net/MSF.556-557.545.

Anastasios E. Arvanitopoulos was born in Patras, Greece, in May 1985. He received the Diploma degree in electrical and computer engineering from the University of Patras, Patras, in 2011. He is currently pursuing the Ph.D. degree with the Research Institute for Future Transport and Cities, Coventry University, Coventry, U.K.

His current research interests include wide bandgap (WBG) power semiconductor devices for high-performance electronics in electric vehicles (EVs).

Marina Antoniou received the B.A. and M.Eng. degrees in electrical and information engineering from the University of Cambridge (Trinity College), Cambridge, U.K., in 2005, and the Ph.D. degree in electrical engineering from the University of Cambridge in 2009.

She was a Junior Research Fellow with the Selwyn College, Cambridge. She is currently an Associate Professor with the University of Warwick, Coventry, U.K., and is also affiliated with the U.K. Power Electronics Centre, University of Nottingham, Nottingham, U.K. Her current research interests include power electronics and high-voltage power semiconductor devices.

Mike R. Jennings received the B.Eng. degree in electronics with communications from the University of Wales, Swansea, U.K., in 2003, the B.Eng. degree incorporated a second year (exchange program) of study with the Union College, Schenectady, NY, USA, and the Ph.D. degree from the University of Warwick, Coventry, U.K., in 2008, with a focus on semiconductor device modeling, processing, and characterization, especially in the field of silicon carbide (SiC) power electronics. His Ph.D. thesis was on Novel Contact Formation for 4H-SiC Power Devices.

Samuel Perkins was born in Norwich, U.K., in September 1993. He received the B.Eng. and M.Res. degrees from Coventry University, Coventry, U.K., in 2017, where he is currently pursuing the Ph.D. degree.

His current research interests include wide bandgap (WBG) power semiconductor devices for ultrahigh-voltage applications.

Konstantinos N. Gyftakis (M'11) was born in Patras, Greece, in May 1984. He received the Diploma degree in electrical and computer engineering and the Ph.D. degree in electrical machines condition monitoring and fault diagnosis from the University of Patras, Patras, in 2010 and 2014, respectively.

From 2014 to 2015, he was a Post-Doctoral Research Assistant with the Department of Engineering Science, University of Oxford, Oxford, U.K. He was a Lecturer from 2015 to 2018 and a Senior Lecturer from 2018 to 2019 with the School of Computing, Electronics and Mathematics, Coventry University, Coventry, U.K., where he was an Associate with the Research Institute for Future Transport and Cities.

Philip Mawby (S'85–M'86–SM'01) received the B.Sc. and Ph.D. degrees in electronic and electrical engineering from the University of Leeds, Leeds, U.K., in 1983 and 1987, respectively. His Ph.D. was focused on GaAs/AlGaAs heterojunction bipolar transistors for high-power radio frequency applications at the GEC Hirst Research Centre, Wembley, U.K.

In 2005, he joined the University of Warwick, Coventry, U.K., as the Chair of Power Electronics. He was also with the University of Wales, Swansea, U.K., for 19 years and held the Royal Academy of Engineering Chair for power electronics, where he established the Power Electronics Design Center.

Neophytos Lophitis received the B.A. and M.Eng. degrees and the Ph.D. degree in power devices from the University of Cambridge, Cambridge, U.K., in 2009 and 2014, respectively.

He was a Consultant for Power Microelectronics companies from 2013 to 2015 and a Research Associate in power with the University of Cambridge from 2014 to 2015. In 2015, he joined Coventry University, Coventry, U.K., where he is currently an Assistant Professor of electrical engineering with the School of Computing, Electronics and Mathematics and the Research Institute for Future Transport and Cities.